Talanta 131 (2015) 417–423

Contents lists available at ScienceDirect

Talanta

journal homepage: www.elsevier.com/locate/talanta

A glucose biosensor based on the synergistic action of nanometer-sized TiO_2 and polyaniline

Wenwei Tang [a,*], Lei Li [b], Xinping Zeng [b,*]

[a] Department of Chemistry, Tongji University, Shanghai 200092, China
[b] School of Life Science and Technology, Tongji University, Shanghai 200092, China

ARTICLE INFO

Article history:
Received 25 April 2014
Received in revised form
6 August 2014
Accepted 7 August 2014
Available online 19 August 2014

Keywords:
Amperometric glucose sensor
Polyaniline
n-TiO_2
Direct electron transfer
Linear range
Detection limit

ABSTRACT

Polyaniline/active carbon (PANI) and nanometer-sized TiO_2 (n-TiO_2) were prepared by oxidation and sol–gel methods, respectively, and were then used as a zymophore to modify a glassy carbon electrode (GCE) and a GOx/n-TiO_2/PANI/GCE sensor with a synergistic effect was established. A series of performance evaluations for the modified material and sensor was studied in detail through cyclic voltammetry (CV) and a chronoamperometry (CA) method. The results showed that the sensor had a good response to glucose and that the electron of the GOx molecule was transferred directly onto the sensor, and a linear relationship between the GOx redox peak current and the sweep speed was found. The apparent transmission speed constant, *k*, for dissimilar electrode charges was 1.35 s^{-1}, 95% of the maximum steady current for the GOx/n-TiO_2/PANI/GCE sensor could be reached in 10 s, the linear range of the detected glucose concentration was from 0.02 mM to 6.0 mM, the sensitivity was 6.31 μA mM^{-1} cm^{-2}, and the limit of detection was 18 μM. The sensor had good selectivity and stability and could be maintained at 82% of the initial activity for 30 days.

1. Introduction

Diabetes mellitus is a serious disease that is harmful to human health, and currently, the effective way to treat it is to severely restrict the diet and control the blood sugar. The blood sugar content is the objective indicator for diabetes mellitus, and it is therefore of great significance to establish a quick, efficient, and inexpensive detection method for glucose. The development of a glucose sensor meets this developmental requirement. Conductive polymer and nanometer-sized materials have received much attention due to their good electrical conductivity, large specific surface area, and small size. Both of these materials have broad application in biosensors.

Nanometer-sized TiO_2 (n-TiO_2), a new inorganic material with a special crystal structure, has been used to affix to biomacromolecules such as enzymes to achieve good biocompatibility and electron transfer ability. n-TiO_2 therefore has a good prospective application in the area of bioelectrochemistry. Li et al. accomplished the fixation and the direct electron transfer process of myohemoglobin, hemoglobin, and cytochrome C to a nanometer-level TiO_2 membrane [1,2]. Zhang et al. prepared a glucose sensor with a detection limit of 0.1 μM by using a multi-walled carbon nanotube/n-TiO_2/gold nanoparticle to modify a GCE [3]. Li et al. made a direct electron transfer of GOx happen on the electrode surface by using mesoporous n-TiO_2/multi-walled carbon nanotube material [4].

Polyaniline, when used as a typical conducting polymer to establish an enzyme-type sensor, has been a topic of intense research interest over the past few years. Due to the conjugated structure that exists in the polyaniline molecule, the electron has a high degree of transferability. In polyaniline, “mixing” could change its electronic structure, magnetic properties, optical properties, electrical conductivity, and structural features remarkably [5]. Lee et al. modified the GOx with functionalized polyaniline and a multiwalled carbon nanotube and accomplished the direct electrochemistry of an enzyme sensor [6]. Dhand et al. found that the GOx showed good electrochemical activity after being wrapped by nanoscale electro-deposited polyaniline, which indicated that the polyaniline has good biocompatibility [7]. Zhai et al. prepared a highly sensitive glucose enzyme sensor based on Pt nanoparticles–polyaniline hydrogel heterostructures, which exhibited unprecedented sensitivity, as high as 96.1 μA mM^{-1} cm^{-2}, with a linear range of 0.01–8 mM, and a low detection limit of 0.7 μM [8].

Polyaniline/active carbon (PANI) and n-TiO_2 were prepared by oxidation and sol–gel methods, respectively, and they were then used to co-modify the electrode surface. By utilizing the good electrical conductivity and the effects of the small sizes of the two

* Corresponding authors.
E-mail addresses: tangww@tongji.edu.cn (W. Tang), zengxp@tongji.edu.cn (X. Zeng).

http://dx.doi.org/10.1016/j.talanta.2014.08.019
0039-9140/

types of materials, a amperometric glucose sensor with a synergistic effect was established, and the detection limit, response time, linear detection range, stability, and anti-jamming capability were studied systematically.

2. Experimental

2.1. Main instruments and reagents

The working electrode was a glassy carbon electrode (GCE, GC130, ⌀3 mm) from Tianjin Aidahengsheng Technology Co., Ltd. The aniline, chitosan, and tetra-*n*-butyl titanate were of analytical purity from the Sinopham Chemical Reagent Co., Ltd., and the GOx, uric acid (UA), L-cysteine, and ascorbic acid (AA) were of biochemical purity from Sigma.

2.2. Preparation of n-TiO_2

Five milliliters (mL) of isopropanol was added into 10 mL of tetra-*n*-butyl titanate, and component A was obtained by stirring for 30 min. Component B consisted of 2 mL of distilled water, 2.5 mL of isopropanol, and a small amount of glacial acetic acid. Component C was obtained by adding the appropriate amount of Polyethylene glycol into 2.5 mL of isopropanol. During the stirring process, component B was dropped into solution C first, and component A was then added dropwise to the BC solution. The duration of the reaction was 0.5 h. The solution that was obtained was aged for 1 day, and then a yellow and transparent sol was obtained. Afterwards, the sol was put into a dryer at 80 °C for 10 h. A xerogel was obtained and was then calcined in the muffle furnace at 500 °C for 2 h, resulting in the TiO_2 powder.

2.3. Preparation of the PANI composite material

Aniline monomer (0.9 mL) and the activated carbon powder (0.84 g) were dispersed in 30 mL of a 1 mol L^{-1} hydrochloric acid solution, and N_2 was blown into the solution to deoxidize it for 30 min. After stirring the solution at a constant speed for 1 h, the aniline monomer was uniformly adsorbed onto the AC surface. An appropriate amount of ammonium peroxydisulfate (APS) was added to 20 mL of the 1 mol L^{-1} hydrochloric acid solution. Then, N_2 was blown into the solution, and the APS was dissolved after stirring. The prepared APS hydrochloric acid solution was dropped into the aniline hydrochloric acid solution gradually over 1 h, the reaction temperature was maintained at 0 °C, and the reaction lasted for 5 h with stirring. After the reaction, the product was washed and filtered repetitively with hydrochloric acid, alcohol, and distilled water to eliminate any oligomer that had not reacted or had not reacted completely. After 24 h of drying in a vacuum oven at 60 °C, the PANI composite material with an atrovirens color was obtained. The optimum molar ratio of AC:ANI:APS for the PANI material was 7:1:1.

2.4. Preparation of the GOx/n-TiO_2/PANI/GCE

Electrode Pre-treatment: Alumina powder with particle diameters of 0.3 μm, 0.1 μm, and 0.05 μm was put on a polishing cloth and soaked in distilled water. The form of the GCE in the alumina powder turbid liquid was the "8" type. The electrode was then polished, and the polished electrode was placed in nitric acid aqueous solution with a volume ratio of 1:1 for 20 min. The electrode was washed with distilled water and alcohol, and the electrode underwent distilled water ultrasonic cleaning. The treated electrode was scanned by cyclic voltammetry (CV) in a solution of 0.1 M KCl and 5 mM $K_3[Fe(CN)_6]$, as $\Delta E_p < 80$ mV, and the electrode was taken out, re-washed with the distilled water, and preserved.

Dispersion of the modified material: PANI or n-TiO_2 powder (1 mg) was put into a 0.5% chitosan solution respectively, and then dispersed uniformly in the chitosan solution after being treated with ultrasound.

Preparation of the GOx solution: Two milligrams of GOx and 15 mg of BSA was placed in 200 μL of standard phosphate buffer, which was then vibrated until the GOx was well distributed and placed in a refrigerator.

PANI/GCE or n-TiO_2/GCE: PANI dispersion (6 μL) or n-TiO_2 dispersion (6 μL) was coated onto the GCE surface respectively, and dried with infrared irradiation.

n-TiO_2/PANI/GCE: 6 μL of the n-TiO_2 dispersion liquid was dropped and coated onto the PANI/GCE surface and dried with infrared irradiation.

GOx/n-TiO_2/PANI/GCE: An appropriate amount of GOx solution and 2.5% glutaraldehyde were rapidly mixed by the glutaraldehyde crosslinking method. The mixture above (6 μL) was quickly placed onto the n-TiO_2/PANI/GCE, dried in the air, and put in the refrigerator at 4 °C for 1 h to complete the GOx and glutaraldehyde crosslinking. The modified electrode was taken out, dried in the air, and preserved in the refrigerator at 4 °C.

2.5. Characterization and detection method

The n-TiO_2 and PANI materials were characterized using SEM, XRD, and electrochemical methods. The preparation method for SEM was that PANI dispersion (6 μL) or n-TiO_2 dispersion (6 μL) was coated onto the GCE surface respectively, and dried with infrared irradiation. The modified electrode was tested in a glucosidic or non-glucosidic situation with CV, electrochemical impedance spectroscopy (EIS), and chronoamperometry (CA). The reproducibility and stability of the sensor were also determined.

3. Results and discussion

3.1. Properties of n-TiO_2

3.1.1. SEM characterization

Fig. 1 shows that the prepared TiO_2 reached sizes on the scale of nanometers, which was directly related to the formation of the sol particles and TiO_2 anatase. Thus, the TiO_2 prepared with the sol–gel method could have good electrical conductivity and the metal ion nanometer effect, and could easily be imbedded into the active center of the enzyme molecule.

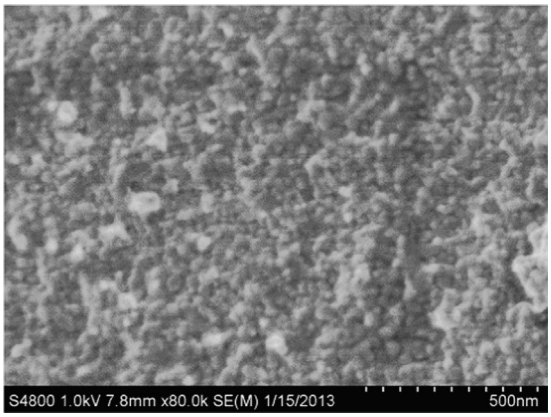

Fig. 1. SEM image of nano-titanium dioxide (80,000 ×).

3.1.2. XRD characterization

The XRD instrument used was a FOUCS D8 X-ray diffractometer from the Bruker Company in Germany, the maximum tube pressure was 40 kV, and the tube current was 40 mA. In the test, the scanning speed was set at 10°/min, and the scanning angle was 10–70°.

An XRD image (Fig. 2) shows that diffraction peaks occurred at 2θ=25.34°, 37.84°, 48.06°, 53.72°, 54.98°, and 62.68°, consistent with the specific diffraction peak of the anatase crystalline-type TiO_2 and indicating that the powder was anatase-phase TiO_2. The size of a crystal in the powder was calculated according to the Scherrer formula

$$D = \frac{K\lambda}{B\cos\theta} \quad (1)$$

where D is the crystal size, K is the Scherrer constant (0.89°), λ is the X-ray wavelength (0.154056 nm), B is the half-height width of the diffraction peak, and θ is the diffraction angle.

According to the crystal face parameters of the characteristic peak (101), the crystal size calculated with Formula (1) was 17 nm.

3.2. Properties of PANI

3.2.1. SEM characterization

An SEM image of PANI (Fig. 3(A) and (B)) shows that the active carbon particle was on the micron scale and that the PANI particles absorbed onto it had diameters of dozens of nanometers, which meant that this composite material could provide more active adsorption sites for the enzyme molecules and could greatly increase the loading capacity of GOx. The electron transfer capability and the bioelectrical activity of the sensor could be improved by combining the good electrical conductivity and biocompatibility of the PANI particle itself.

3.2.2. FTIR characterization

In Fig. 4, the peak at 3448 cm^{-1} corresponds to the stretching vibration absorption peak of N–H, the peak at 1635 cm^{-1} is the deformation vibration absorption peak of N–H, the peak at 1568 cm^{-1} is the vibration absorption peak of C=C in a quinine-type ring, the peak at 1504 cm^{-1} is the vibration absorption peak of C=C in a benzene-type ring, the peak at 1170 cm^{-1} is the vibration absorption peak of −H+N=C related to a quinine-type ring, and the peak at 1068 cm^{-1} is the stretching vibration absorption peak of C–N. The positions of these peaks met the characteristic peak ranges of an amine substance: the stretching vibration absorption peak of N–H was in the range of 3500–3100 cm^{-1}, and the stretching vibration absorption and the deformation vibration peaks of C–N were in the ranges of 1350–1000 cm^{-1} and 1640–1560 cm^{-1}, respectively. These ranges are close to the peak positions in the spectrum of PANI [9], and these results indicated that the polymerization of the aniline molecule occurred during the mixing process.

3.3. Conductivity of n-TiO_2 and PANI

3.3.1. CV during the electrode assembly process

A pair of redox peaks from $[Fe(CN)_6]^{3-/4-}$ via a complete and reversible process were observed on the surface of the bare electrode, as shown in Fig. 5. The redox peak currents of the

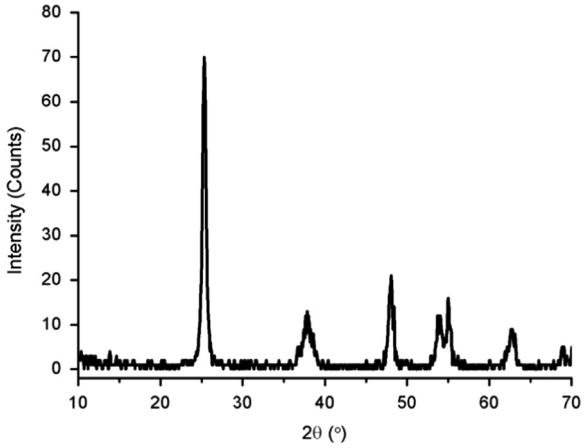

Fig. 2. XRD image of nano-titanium dioxide.

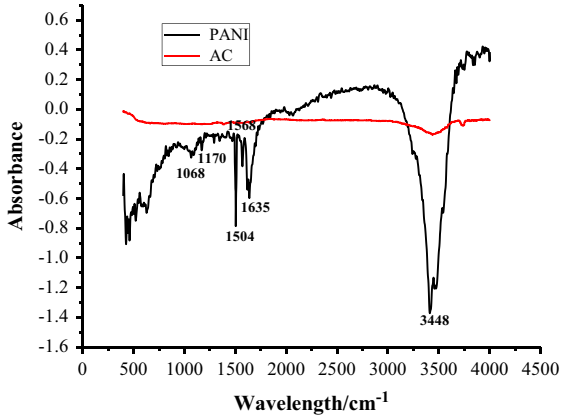

Fig. 4. FTIR spectrum of AC and PANI.

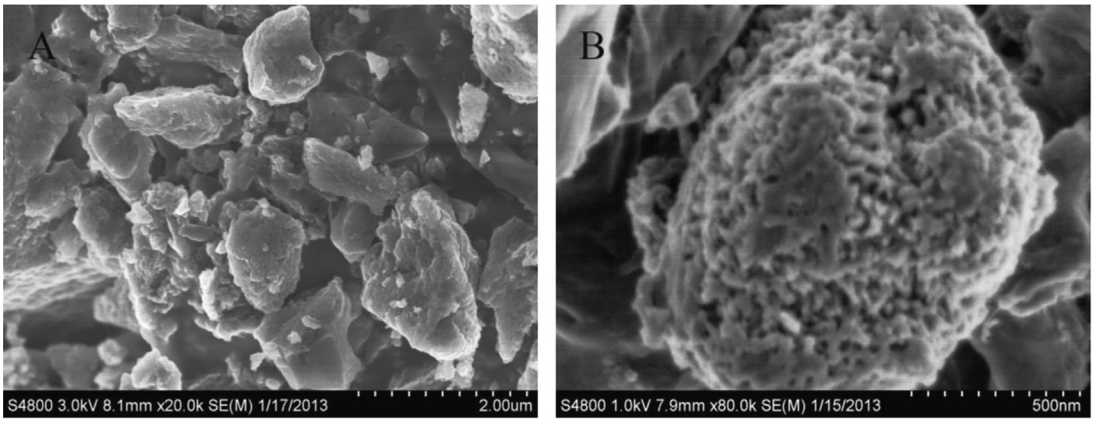

Fig. 3. SEM image of AC and PANI (A: AC, B: PANI).

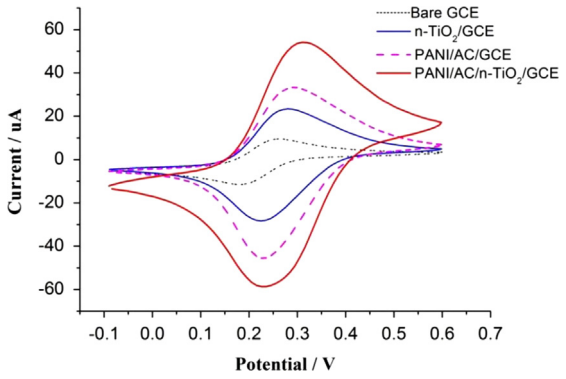

Fig. 5. CV of bare GCE, n-TiO_2/GCE, PANI/GCE, and n-TiO_2/PANI/GCE electrodes in a 1.0 mM $K_3Fe(CN)_6$ solution.

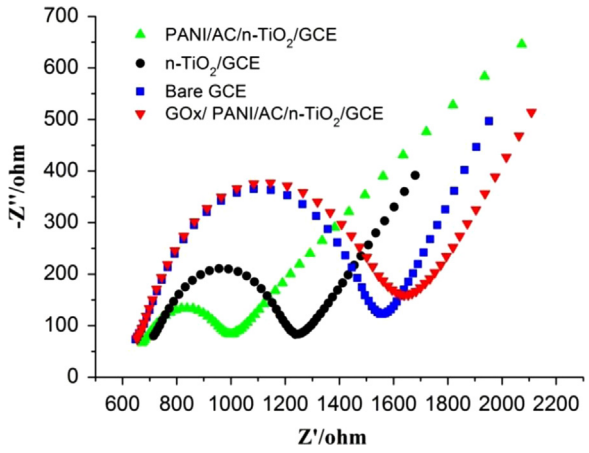

Fig. 6. Electrochemical impedance spectra of bare GCE, n-TiO_2/GCE, n-TiO_2/PANI/GCE, and GOx/n-TiO_2/PANI/GCE electrodes. Supporting electrolyte: 5.0 mM solution of $[Fe(CN)_6]^{3-/4-}$.

electrodes modified by n-TiO_2 and PANI obviously increased to values that were 2 and 3 times the values of the bare electrode, which indicated that the PANI had a better conductivity than the n-TiO_2. For the electrode that was modified by a composite of both the n-TiO_2 and PANI, the redox peak current of $[Fe(CN)_6]^{3-/4-}$ increased to almost six-fold over the bare electrode, which was larger than the sum of the peak currents of the electrodes modified by the two separately. These results indicated that a good synergistic effect occurred when the n-TiO_2 and PANI were combined, and in combination, they could greatly improve the electron transfer ability of the sensor interface.

3.3.2. *EIS of the electrode assembly process*

The surface resistances of the electrodes modified by different materials were different (see Fig. 6); the impedance atlas diameter and the resistance value with the n-TiO_2 and n-TiO_2/PANI modifications were comparatively smaller, which meant that the prepared n-TiO_2 had a good conductivity and that the synergistic effect occurred when it was combined with PANI. The synergistic effect could greatly improve the interfacial electron transfer ability and the redox reaction of the probe on the electrode surface. When the GOx was introduced into the modification, the impedance atlas diameter of the sensor increased greatly again, the main reason being that the fixed GOx is a biomacromolecule with a large resistance value, which demonstrated that the enzyme was successfully assembled on the electrode surface layer-by-layer.

3.4. *Direct electrochemistry of GOx/n-TiO_2/PANI*

Fig. 7 shows that, compared with the bare electrode (a), the current response of the electrode modified by the PANI and n-TiO_2 (b) increased significantly. A pair of unobvious redox peaks of the GOx/n-TiO_2/GCE (c) and the GOx/PANI/GCE (d) electrodes appeared at −0.45 V, which meant that only weak direct electron transfer of the enzyme could occur if the electrode was modified by PANI or n-TiO_2. The electrode that was modified by the composite of PANI and n-TiO_2, and loaded with the enzyme had a pair of very obvious GOx redox peaks (E_{pa} = −0.415 V, E_{pc} = −0.451 V) near −0.45 V, which meant that the GOx had already been successfully modified on the electrode surface and that an obvious direct electron transfer occurred. The reason behind this phenomenon might be that modification with the PANI and n-TiO_2 composite not only provided a large specific surface area, good biocompatibility, and more active center sites for GOx but also helped to decrease the steric hindrance of the enzyme active centers and the electrode surface and made the direct electron transfer of the enzyme occur. Meanwhile, for the sample with the enzyme as the bioactive molecule, its large resistance resulted in a low current response compared with the

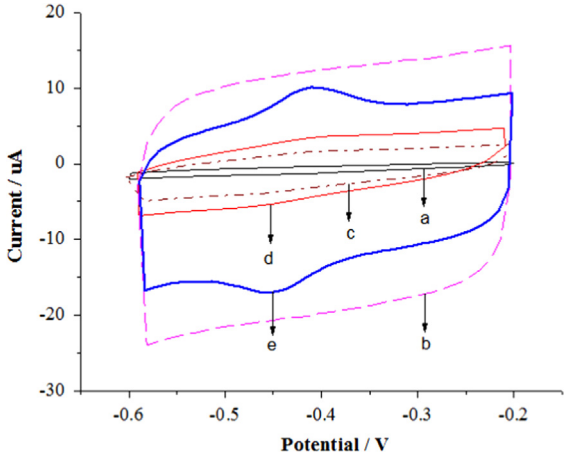

Fig. 7. CV of bare GCE (a), n-TiO_2/PANI/GCE (b), GOx/n-TiO_2/GCE (c), GOx/PANI/GCE (d), and GOx/n-TiO_2/PANI/GCE (e) electrodes in 0.1 M nitrogen-saturated PBS.

sample without modification by the enzyme, which also agreed with the conclusion from the EIS and CV.

The electroactivity density (Γ, mol cm^{-2}) of GOx on the electrode surface was calculated by Formula (2)

$$Q = nFA\Gamma \quad (2)$$

where Q is the total charge quantity (c) through the electrode surface, n is the electron transfer amount, F is Faraday's constant, and A is the electrode surface area (cm^{-2}).

The reduction peak of GOx/n-TiO_2/PANI/GCE under a scanning speed of 100 mV/s was integrated (Fig. 8) according to Formula (2). The degree that the electroactive oxidase covered the electrode surface, Γ, was 2.79×10^{-10} mol cm^{-2}, which was much larger than the theoretical value (2.97×10^{-12} mol cm^{-2}) of the monolayer enzyme on the bare electrode surface (assuming that the long axis of the GOx molecule ($5.5 \times 7.0 \times 8.0$ nm^3) [10] was parallel to the electrode surface). The fact that the actual value was much larger than the theoretical value meant that the GOx on the electrode surface modified the electrode with multiple layers and that direct electron transfer occurred. At the same time, the value was also larger than the coverage density of a fixed enzyme modified by a porous material, such as TiO_2 (2.57×10^{-10} mol cm^{-2}) [11], AuNPs/MWCNTs/PVA (2.56×10^{-10} mol cm^{-2}) [12], SWCNT/chitosan (1.3×10^{-10} mol cm^{-2}) [13], PEDOT-NiO NS (1.56×10^{-10} mol cm^{-2}) [14], CdS (1.54×10^{-11} mol cm^{-2}) [15],

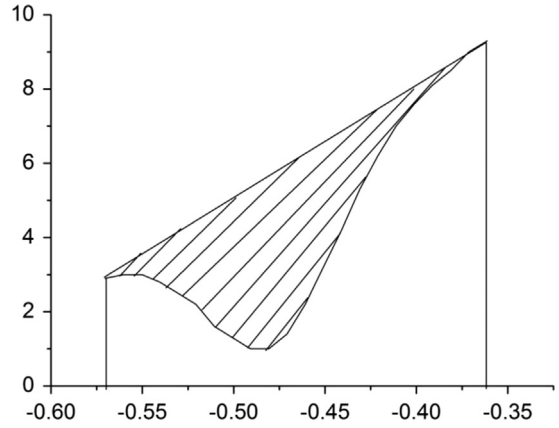

Fig. 8. Integration of the reduction peak at 100 mV s^{-1}.

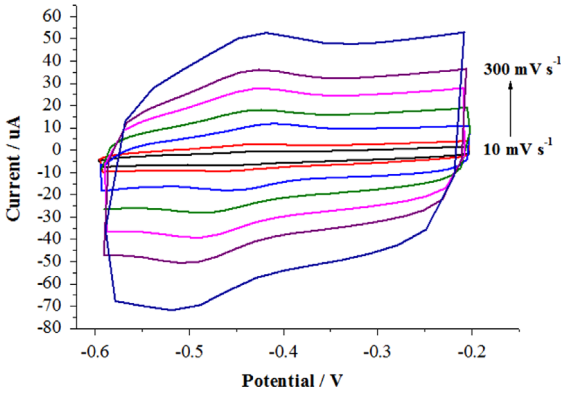

Fig. 9. CV of the GOx/n-TiO_2/PANI/GCE modified electrode in 0.1 M nitrogen-saturated PBS at scan rates of 10, 20, 50, 100, 150, 200, and 300 mV s^{-1} from inner to external.

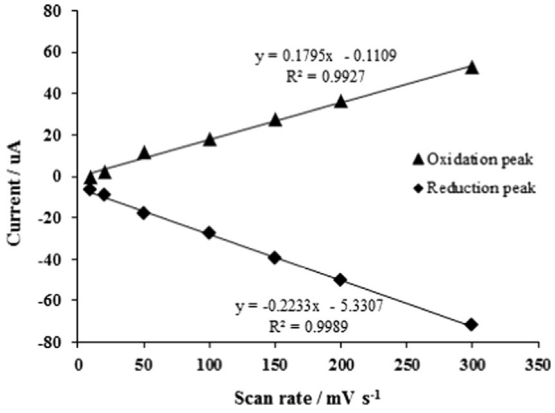

Fig. 10. Values of the enzyme peak current as it changed with the scanning speed.

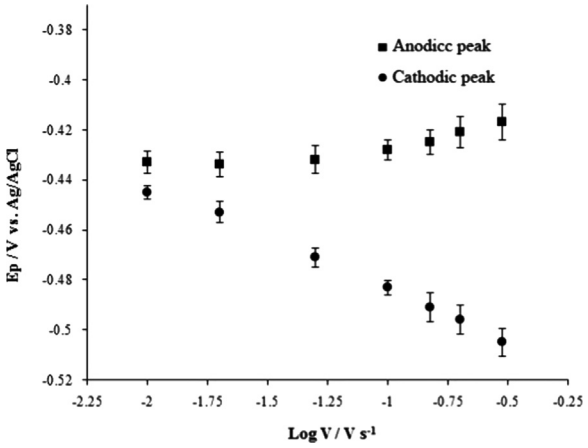

Fig. 11. Plots of the anodic and cathodic peak potentials (E_p vs. log v).

and AuNPs (9.8×10^{-12} mol cm^{-2}) [16], indicating that the n-TiO_2 and PANI composite had good biocompatibility and could maintain the microstructure and the bioelectrical activity of the GOx.

3.5. CVs of GOx/n-TiO_2/PANI/GCE under different scanning speeds

Fig. 9 shows that the redox peak current value of GOx increased as the scanning speed increased from 10 mV s^{-1} to 300 mV s^{-1}, and a good linear relationship is demonstrated (Fig. 10). The peak redox current value had a linear relationship with the scanning speed, V, and the R^2 of the reduction peak value reached 0.999, which meant that the process was controlled by the adsorption reaction of the redox material on the electrode surface and not by the diffusion process [17,18]. The GOx was also demonstrated to be well-modified on the electrode surface and formed a CV graph that was similar to the adsorption reactant.

The data in Fig. 11 are from Fig. 9 and show the redox peak potential change of GOx at different scanning speeds. This electrochemical process at the surface can also be described by the Laviron Equation [19,20]

$$E_{pc} = E^{o'} - \frac{2.3RT}{\alpha nF}\left\{\log\frac{\alpha Fn}{RT} + \log[v] - \log[k]\right\} \quad (3)$$

$$E_{pa} = E^{o'} - \frac{2.3RT}{(1-\alpha)nF}\left\{\log\frac{(1-\alpha)Fn}{RT} + \log[v] - \log[k]\right\} \quad (4)$$

$$\log k = \alpha\log(1-\alpha) + (1-\alpha)\log\alpha - \log\left(\frac{RT}{nFv}\right) - \frac{\alpha(1-\alpha)nF\Delta E_p}{2.3RT} \quad (5)$$

where E_{pa} and E_{pc} represent the positive electrode and the reduction peak potentials, respectively, $\Delta E_p = E_{pa} - E_{pc}$, α is the negative electrode transfer coefficient, v is the scanning speed (V s^{-1}), k is the apparent dissimilar charge transfer speed constant (s^{-1}), n is the electron transfer number, R is the ideal gas constant, and T is the reaction temperature.

According to the locus change slope of the redox peak in Fig. 11 (the linear equation was $y=-0.040x-0.524$, $R^2=0.9917$) and Formula (3), α was deduced to be 0.365. According to the ΔE_p and log v curves from Formula (5) in Fig. 12, the apparent dissimilar charge transfer speed constant, k, was deduced to be 1.35 s^{-1} ($n=4$), which was smaller than that for the electrode modified by the CNT/GOx (1.6 s^{-1}) [21] but larger than that for GC/CNT/Au/PDDA-GOD (1.01 s^{-1}) [22], this finding indicated that the composite modification with PANI and n-TiO_2 had a good charge transfer ability.

3.6. Current response of GOx/n-TiO_2/PANI/GCE to glucose

3.6.1. Voltamperometric response

Without the addition of glucose, the reduction peak of the enzyme could be observed at −0.47 V, as shown in Fig. 13, and the peak current decreased with an increase in the glucose concentration. As the glucose concentration increased, the glucose entered the enzyme active center competitively and accelerated the transformation of GOx (FAD) to GOx ($FADH_2$), directly resulting in a decrease in the reduction current in the system.

The change in the sensor reduction peak value with the glucose concentration is described in Fig. 14, which shows that the cathode current decreased greatly over the glucose concentration range of

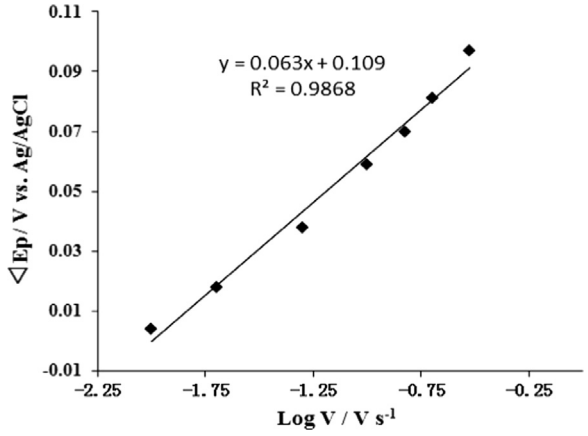

Fig. 12. Plots of the anodic and cathodic peak potentials (E_p vs. log v).

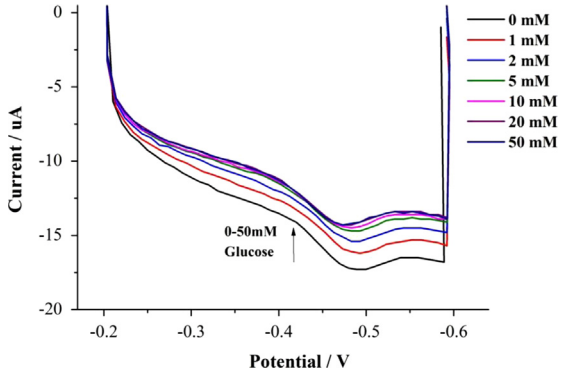

Fig. 13. Reduction current curve of the GOx/n-TiO_2/PANI/GCE biosensor in a 0.1 M solution of nitrogen-saturated PBS (pH=7.0) with different glucose concentrations.

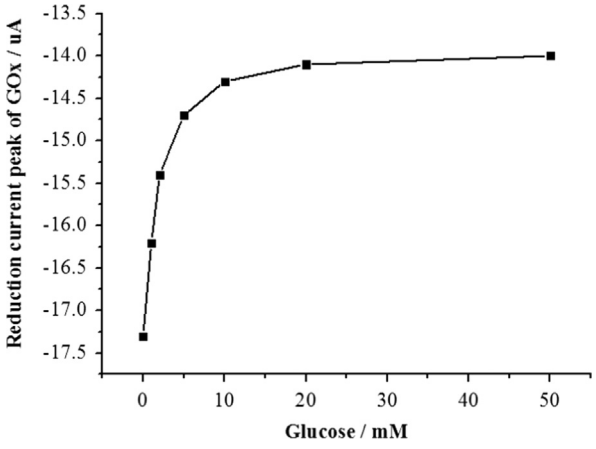

Fig. 14. Plot of the reduction current peak of GOx vs. the glucose concentration.

0–10 mM. As the glucose concentration continued to increase, the FAD and $FADH_2$ transformation of the active centers gradually tended to be saturated, and the current decrease tended to smooth out. This finding is similar to the results reported by Si et al. [23], which meant that the GOx participated in the direct electron transfer on the electrode surface and the glucose molecule directly reacted catalytically. Thus, the sensor can be classified as of the third generation.

3.6.2. Amperometric response

Figs. 15 and 16 show that the current could reach 95% of the maximum stable current in 10 s, indicating that the response of

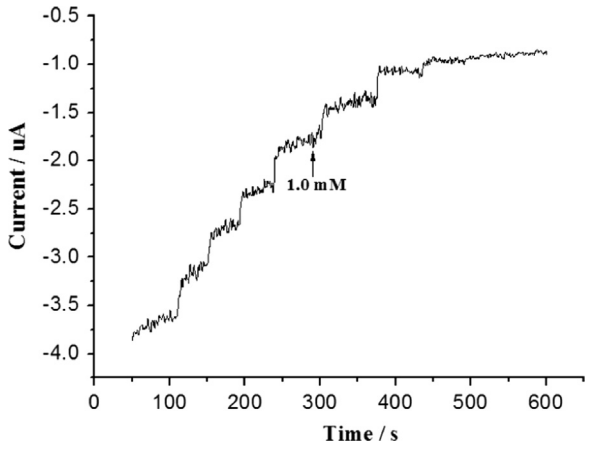

Fig. 15. Amperometric response of the GOx/n-TiO_2/PANI/GCE-modified electrode in a stirred 0.1 M PBS solution (pH=7.0) for successive additions of 1.0 mM glucose at −0.45 V.

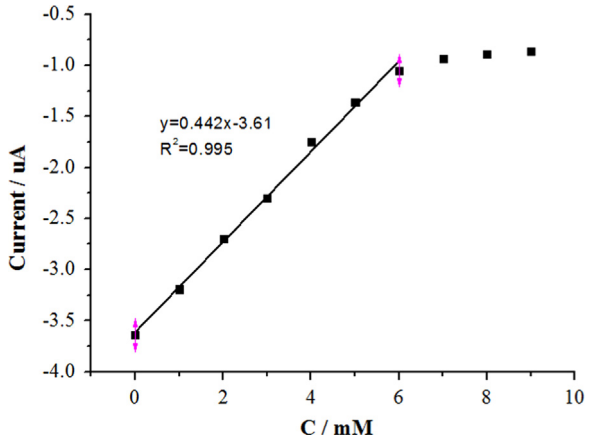

Fig. 16. Calibration curve (current vs. glucose concentration) obtained from the amperometric response.

the sensor was fast and that the GOx modified on the surface could effectively catalyze the glucose molecule reduction reaction. The linear range of the detected glucose concentration was from 0.02 mM to 6.0 mM, the linear equation was $I=0.442x-3.61$, and the correlation coefficient was 0.995. A 1.0 mM increase in glucose resulted in an approximately 442 nA decrease in the cathode current, and the cathode current reached a minimum current value of −1.05 μA. The sensitivity of the sensor was approximately 6.31 μA mM^{-1} cm^{-2}, and the detection limit of the sensor estimated by the triple SNR formula ($s=2.4\times10^{-9}$) was 18 μM.

3.7. Anti-interference, repeatability, reproducibility and stability of GOx/n-TiO_2/PANI/GCE

The current changes following the addition of 2.0 mM UA, L-cysteine, and AA are shown in Fig. 17, and the changes are negligible compared with the current change brought about by the addition of a glucose solution of the same concentration. The GOx/n-TiO_2/PANI/GCE electrode had better selectivity and anti-jamming capability than other electrodes because the sensor measured the glucose with a reduction method at a low working voltage (−0.45 V) and could avoid the interference by the high voltage oxidation of an interfering substance.

We put eight sensors in PBS solution, which had a glucose concentration of 2.0 mM, to perform current tests. The relative standard deviation (RSD) of the biosensor was 2.66%, which has been shown to be an acceptable reproducibility. After the

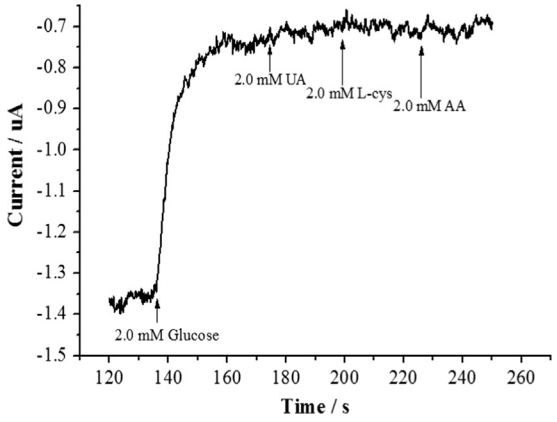

Fig. 17. Effect of possible interferences in the biosensor. The arrows show the moment at the injection of each of the interfering compounds: 2.0 mM glucose, 2.0 mM UA, 2.0 mM L-cysteine, and 2.0 mM AA in a stirred solution of 0.1 M PBS (pH=7.0) at −0.45 V.

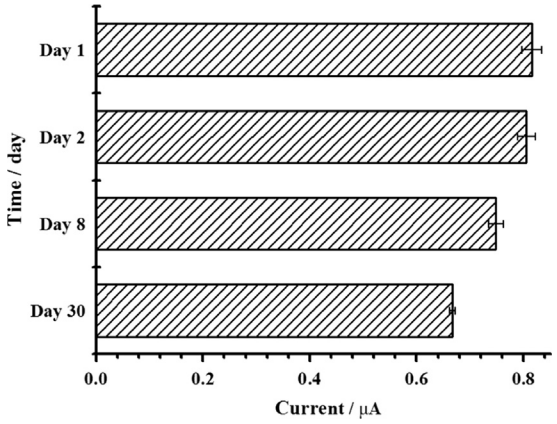

Fig. 18. Stability of the modified biosensors over a storage period of four weeks.

experiment, the sensor was preserved at 4 °C and detected at different times. As shown in Fig. 18, the electrode response did not obviously change in the beginning after 2 days. After the electrode was preserved for 1 week, the electrode current response reached 91.8% of the original, and after 30 days, the response reached 81.7% of the original. In Fig. 18, RSD for five successive measurements was small and the repeatability was good, all which meant that the GOx/n-TiO_2/PANI/GCE electrode had good stability. The main reasons for this outcome are as follows: first, the chitosan could wrap and fix the PANI and n-TiO_2 onto the electrode surface well, and the particle combination could improve the electrode conductivity and increase the solid loading of the enzyme. Second, the glutaraldehyde crosslinking method is a classic covalence enzyme connection method, which can effectively prevent enzyme loss. In addition, the average life expectancy of the working electrode is 70 days.

4. Conclusions

PANI and n-TiO_2 were prepared by oxidation and sol–gel methods, respectively. The CV and EIS both showed that the two were good conductive materials. The synergistic effect occurred when the electrode was modified by the composite of the two, and the electron transfer ability was greatly improved. A amperometric glucose sensor was established with the PANI composite and n-TiO_2 as the GOx carrier. This sensor had a good response to the glucose, the electron of the GOx molecule was transferred directly onto the sensor, and a linear relationship between the GOx redox peak current and the sweep speed was found. The apparent transmission speed constant, k, for the dissimilar electrode charges was 1.35 s^{-1}, 95% of the maximum steady current for the GOx/n-TiO_2/PANI/GCE sensor could be reached in 10 s, the linear range of the detected glucose concentration was from 0.02 mM to 6.0 mM, the linear equation was $I=0.442x-3.61$, and the correlation coefficient was 0.995. The sensitivity was 6.31 μA mM^{-1} cm^{-2}, and the limit of detection was 18 μM. The sensor had good selectivity and stability, and it could be maintained at 82% of the initial activity for 30 days.

Acknowledgments

This work was supported by the National Natural Science Foundation of China (No. 21277098), the Natural Science Foundation of Shanghai (No. 10ZR1432500), and the Shanghai Municipal Commission of Economy and Informatization (No. 12CH-12).

Reference

[1] Y. Zhang, R.L. He, N.E. Hu, Electrochim. Acta 49 (2004) 1981–1988.
[2] M. Addamo, V. Augugliaro, A.D. Paola, E. García-López, V. Loddo, G. Marcì, R. Molinari, L. Palmisano, M. Schiavello, J. Phys. Chem. B 108 (2004) 3303–3310.
[3] M.H. Zhang, R. Yuan, Y.Q. Chai, W.J. Li, H. Zhong, C. Wang, Bioprocess Biosys. Eng. 34 (2011) 1143–1150.
[4] J.H. Li, D.Z. Kuang, Y.L. Feng, F.X. Zhang, M.Q. Liu, Microchim. Acta 176 (2012) 73–80.
[5] A.G. Macdiarmid, A.J. Epstein, Synth. Met. 69 (1995) 85–92.
[6] K.P. Lee, S. Komathi, N.J. Nam, A.I. Gopalan, Microchem. J. 95 (2010) 74–79.
[7] C. Dhand, G. Sumana, M. Datta, B.D. Malhotra, Thin Solid Films 519 (2010) 1145–1150.
[8] D.Y. Zhai, B.R Liu, Y. Shi, L.J. Pan, Y.Q. Wang, W.B. Li, R. Zhang, G.H. Yu, ACS Nano 7 (2013) 3540–3546.
[9] W. Qiu, Master Degree thesis, Chongqing University, China, 2008.
[10] M. Hartmann, Chem. Mater. 17 (2005) 4577–4593.
[11] S.J. Bao, C.M. Li, J.F. Zang, X.Q. Cui, Y. Qiao, J. Guo, Adv. Funct. Mater. 18 (2008) 591–599.
[12] H.F. Zhang, Z.C. Meng, Q. Wang, J. Zheng, Sens. Actuators B Chem. 158 (2011) 23–27.
[13] Y. Zhou, H. Yang, H.Y. Chen, Talanta 76 (2008) 419–423.
[14] C.X. Guo, C.M. Li, Phys. Chem. Chem. Phys. 12 (2010) 12153–12159.
[15] Y.X. Huang, W.J. Zhang, H. Xiao, G.X. Li, Biosens. Bioelectron. 21 (2005) 817–821.
[16] S.Q. Liu, H.X. Ju, Biosens. Bioelectron. 19 (2003) 177–183.
[17] A.J. Bard, L.R. Faulkner, Electrochemical methods: Fundamentals and applications, John Wiley & Sons, New York, 2001.
[18] Y.H. Wu, S.S. Hu, Bioelectrochemistry 70 (2007) 335–341.
[19] R.W. Murray, A.J. Bard, Electroanalytical Chemistry, Marcel Dekker, New York, 1984.
[20] E. Laviron, J. Electroanal. Chem. 101 (1979) 19–28.
[21] Y.D. Zhao, W.D. Zhang, H. Chen, Q.M. Luo, Anal. Sci. 18 (2002) 939–941.
[22] Y.L. Yao, K.K. Shiu, Electroanalysis 20 (2008) 1542–1548.
[23] P. Si, S. Ding, J. Yuan, X.W. Lou, D.H. Kim, ACS Nano 5 (2011) 7617–7626.